Investigation of self-powered gamma flux detectors with Lead(II) oxide serving as both emitter and insulator

H. Shi[1], S. Yue[2], G. Jonkmans[2], B. Sur[2] and John Hilborn[2]

[1]Deep River Science Academy, Deep River, Ontario, Canada
[2]Atomic Energy of Canada Limited, Chalk River, Ontario, Canada

Abstract

The use of Lead(II) oxide as the electron-emitting component and the insulating component of self-powered flux detectors is a concept that had not been previously explored. Detectors constructed from various combinations of electrodes (stainless steel, Al, Pb, and W) and insulating materials (Al_2O_3 and PbO) were irradiated in a 427 *Gy/h* gamma field. Although high gamma sensitivities were achieved, PbO did not prove to be a strong emitter of gamma-induced electrons. Nevertheless, PbO did serve as a better insulator than one that is currently in use, namely alumina.

1. Introduction

With the development of large nuclear reactors, it has become imperative to use in-core instrumentation to determine the power distribution within a reactor core. To address the evolving needs of reactor technologies, self-powered flux detectors (SPFDs) were designed to measure the neutron flux inside of a reactor core without an external power source [1]. These in-core flux detectors are widely used for flux mapping, spatial regulation, and safety shutdown systems [2]. A CANDU-sized reactor may have over 100 SPFDs positioned in its interior [3].

The SPFD is a three-part coaxial assembly consisting of an inner (core) electrode and an outer (sheath) electrode separated by an insulator sandwiched in between. The two electrodes are connected through an external circuit and ammeter to allow radiation-induced currents to flow between the core and sheath. In a fission reactor, neutrons and gamma photons can induce currents in SPFDs by the following interactions:

1. **(n, β)** A neutron may be captured by an atomic nucleus in the detector and undergo beta-decay, resulting in one liberated electron per neutron capture.
2. **(n, γ, e)** A neutron captured by a nucleus in the detector may be accompanied by an immediate emission of gamma rays. These gamma rays are able to interact with electrons via Compton scattering and the photoelectric effect, resulting in several liberated electrons per neutron capture.
3. **(γ, e)** Gamma rays produced directly through nuclear fission may interact with electrons in the detector via Compton scattering, the photoelectric effect, and pair production, resulting in several liberated electrons per incident photon.

Traditionally, materials that make up the different components of the detector are chosen so that the above interactions occur predominantly in the core and that the liberated electrons settle in the sheath. For this reason, the terms “emitter” and “collector” have been coined for the core and sheath, respectively. During irradiation, electrons are lost by the emitter and are captured by the collector, thereby producing a potential difference between the two electrodes. Due to the difference in electric potential, electrons flow back from the collector to the emitter through the external circuit and ammeter, generating a small, detectable current. The current, thus measured, is proportional to the neutron or gamma flux in the reactor core.

Despite the widespread use of SPFDs in CANDU reactors, one inherent issue had always accompanied the current-inducing mechanism in these instruments. The (n, β) and (n, γ, e) interactions that occur within a detector transmute the emitter material to one that is usually less sensitive to neutrons, thereby reducing the overall detector sensitivity over time. Table 1 lists the rates at which detectors with various emitters lose their sensitivity (burn-up) [4].

Table 1: Burn-up characteristics of various detectors in neutron flux of $10^{14}\, n \cdot cm^{-2} \cdot s^{-1}$

Emitter Material	Neutron Cross Section (barn)	Burn-up Rate (% per annum)
Zirconium	0.05	0.001
Cerium	0.58	0.2
Vanadium	4.9	1.6
Platinum	29	1.8
Cobalt	37	11
Rhodium	145	32
Tantalum	8500	100

The damage caused by neutrons is proportional to the macroscopic neutron cross-section of the emitter material and the neutron flux [5]. Although some detectors in Table 1 react minimally with neutrons and undergo extremely slow burn-up, their output currents are consequently very limited. Therefore, a compromise between the output signal and burn-up rate must be made when employing detectors for practical purposes. Currently, only Vanadium, Inconel, Platinum, and Platinum-clad detectors are used in CANDU reactors. Vanadium and Inconel detectors rely nearly entirely on (n, β) and (n, γ, e) interactions as sources of current, whereas the Platinum detectors depend on (γ, e) interactions to produce up to 40% of the total current, with the remaining 60% contributed by the two aforementioned means [2]. A solution that avoids the perpetual replacement or recalibration of detectors due to burn-up has yet to be found.

1.1 Proposed solution

The present study intends to explore the feasibility of a SPFD that produces a current utilizing (γ, e) interactions alone. In such a detector, Lead (Pb) is the ideal material for the emitter because its high electron density and low neutron cross-section (0.49 millibarns) produces high gamma interaction rates and a low burn-up rate [6]. Pb detectors, however, cannot be deployed in a high-power reactor because Lead metal has a melting point of approximately

300°C, and the maximum operating temperature of a CANDU reactor could reach as high as 310°C [7]. Consequently, litharge (a form of Lead(II) oxide – PbO) is chosen as a substitute for the emitter material. PbO, with its large band gap, is a fairly non-conducting material, so it is integrated as the insulating layer of the detector rather than the core. The purpose of present experiment is twofold: (1) to examine the effects of a Lead-based emitter, and (2) to investigate the effects of using PbO as the insulator. To the best of the author's knowledge, no prior study had been conducted to assess the latter. In this study, the performance of a PbO-insulated detector is examined and compared with that of detectors assembled using other materials.

2. Methodology

2.1 Detector design

Each detector consists of insulating powder packed densely inside of a metal tube (sheath) with a metal rod (core) held at the center in a coaxial geometry. The assembly is held together by epoxy applied at both ends. Finally, an 8-m long, low noise RG-174 coax cable was electrically connected to the detector on one end. A male BNC connector was attached to the other end of the coax cable.

A total of six sets of detectors were constructed. Table 2 summarizes the constituents and the dimensions of each detector in sets 1 through 5. The design of set 1 detectors was unique in that the detector and the coax cable were two separate pieces joined by a BNC connection, whereas the coax cable was directly attached to the detector in all other sets. Set 4 detectors also deviate slightly from the basic detector design due to a Teflon sleeve that was slipped over the metal core. These modifications were intended to simplify construction and not to alter detector characteristics to any significant extent.

Set 6 detectors were produced under an alternate design. The "Thermo" detector consisted of a 72 *inch*, 1 *mm* O.D., ungrounded, K-type thermocouple that was curled into a 6.35 *mm* I.D. coil. The final length of the detector was approximately 90 *mm*. The leads were electrically connected to the center wire of the RG-174 cable and the sheath was connected to the braid of the cable. Detectors W-94 and W-76 were built by enveloping pieces of 3.97 *mm* O.D. Tungsten welding rod (94 *mm* long and 76 *mm* long, respectively) in heat shrink, and then spiral wrapping three layers of Aluminum foil over them. An additional layer of heat shrink was wrapped over top to hold the assembly tightly together. The Tungsten was electrically connected to the center wire of the RG-174 cable, and the Aluminum foil was joined to the braid of the cable. Detector Pb-42 was constructed in the same manner using a 42 *mm* long, 3.175 *mm* O.D. Lead wire instead of Tungsten.

2.2 Irradiation and data collection

Before irradiation, the sheath and core of each detector were shorted for several hours to ensure that both electrodes possessed the same initial charge. The shorting cable was only removed when a detector was to be connected to the measuring equipment.

All detectors were irradiated in gamma cells located in Chalk River Laboratories. Set 1 detectors were irradiated in a Gammacell 220 with a gamma field of 300 *Gy/h* (30 *kRad/h*), while all other detectors were irradiated in a different Gammacell 220 with field strength of 427 *Gy/h* (42.7 *kRad/h*).

FEMTO's DLPCA-200 transimpedance amplifier was used to measure the small currents generated by each detector. Measurements were initially taken under the 10^{10} *V/A* gain setting through a low-pass filter (10 *Hz*). If the input current exceeded the maximum input limit of the initial gain, the multiplier was reduced by factors of 10 until readings could be made.

The amplifier was given sufficient time to "warm up" before data collection began to minimize the potential effects of temperature-dependent drift. Real-time data collection commenced after each detector was placed into the irradiation chamber of the gamma cell. Data were recorded for 5 minutes with the chamber located outside of the irradiation zone and for another 5-10 minutes with the irradiation chamber lowered into the irradiation site.

The insulation resistance of detectors were determined by I-V (current-voltage) curves generated by the Keithley 6487 PicoAmmeter/Voltage Source. The Keithley picoammeter was used to bias detectors from –1.0 *V* to + 1.0 *V* in 0.1 *V* increments and to record the current produced at each interval. Applying Ohm's Law, the internal resistance of each detector in its self-powered state should equal the inverse slope of the curve at V=0.

3. Results and discussion

3.1 Source of photocurrent

Traditionally, SPFDs produced only positive signals, as the current flows from core to sheath (i.e. electrons deposited in the sheath return to the core through the external circuit). As shown in Figure 1, negative currents were achieved by detectors in sets 1, 2, 3, and 5, indicating electron flow in the opposite direction. The values in Figure 1 correspond to the difference between the currents just before the irradiation chamber was lowered and the current observed immediately after the chamber was completely lowered.

All negative signals were produced by detectors with similar electrodes (i.e. the same material). By virtue of the geometry of the detector, the outer electrode should capture more electrons from the insulator than the inner electrode, thus producing a positive current. However, the electron density of stainless steel is nearly twice as large as that of PbO and nearly 10 times larger than that of Al_2O_3, as calculated by Equation 1. Therefore, stainless steel rather than the insulators, as originally intended, acted as the principle emitter of the detectors. Because the larger outer electrode could effectively emit more electrons than the inner electrode, more electrons would be deposited in the core from the sheath rather than the reverse.

Table 2: Description of Experimental Detectors from Sets 1-5

Set	Detector Identification	Sheath O.D. (mm)	Core O.D. (mm)	Insulator Thickness (mm)	Length (mm)	Emitter	Insulator	Sheath
1	1A	6.35	0.89	1.84	300	Stainless Steel	Air	Stainless Steel
	1B	6.35	0.89	1.84	300	Stainless Steel	Al_2O_3 (un-dried)	Stainless Steel
	1C	6.35	0.89	1.84	300	Stainless Steel	PbO	Stainless Steel
2	2A	6.35	0.89	1.84	100	Stainless Steel	Air	Stainless Steel
	2B	6.35	0.89	1.84	100	Stainless Steel	Al_2O_3 (un-dried)	Stainless Steel
	2C	6.35	0.89	1.84	100	Stainless Steel	PbO	Stainless Steel
	2D	6.35	0.89	1.84	100	Stainless Steel	Al_2O_3 (dried†)	Stainless Steel
3	3A	6.35	3.175	0.70	100	Stainless Steel	Air	Stainless Steel
	3B	6.35	3.175	0.70	100	Stainless Steel	Al_2O_3 (un-dried)	Stainless Steel
	3C	6.35	3.175	0.70	100	Stainless Steel	PbO	Stainless Steel
	3D	6.35	3.175	0.70	100	Stainless Steel	Al_2O_3 (dried†)	Stainless Steel
4	4A	6.35	3.175	0.70	100	Lead	Air*	Aluminum
	4B	6.35	3.175	0.70	100	Lead	Al_2O_3 (un-dried)*	Aluminum
	4C	6.35	3.175	0.70	100	Lead	Al_2O_3 (dried†)*	Aluminum
	4D	6.35	3.175	0.70	100	Lead	Al_2O_3 (dried†)*	Aluminum
	4E	6.35	3.175	0.70	100	Stainless Steel	PbO	Aluminum
5	5A	3.76	2.38	0.31	100	Stainless Steel	PbO	Stainless Steel
	5B	3.76	1.73	0.635	100	Stainless Steel	PbO	Stainless Steel
	5C	3.76	1.73	0.635	100	Stainless Steel	PbO	Stainless Steel
	5D	3.76	2.38	0.31	100	Stainless Steel	Al_2O_3 (dried†)	Stainless Steel
	5E	3.76	1.73	0.635	100	Stainless Steel	Al_2O_3 (dried†)	Stainless Steel
	5F	3.76	1.73	0.635	100	Stainless Steel	Al_2O_3 (dried†)	Stainless Steel

† Baked in a drying oven at 110°C for 5 days; * Thin Teflon sleeves in addition to powdered insulator.

$$electron\ density = \frac{\rho N_A}{M} \cdot \sum fZ \qquad (1)$$

Where f is the percentage composition of each element in the compound,
Z is the atomic number of the element,
ρ is the density of the compound,
M is the atomic weight of the compound, and
N_A is Avogadro's constant.

The positive signals observed were produced by detectors that contained dissimilar electrodes. The inner electrodes of these detectors (stainless steel, Pb, W) all had much higher electron density than the outer electrode (Al). Thus, it should be expected that more electrons are emitted from the core and become deposited in the sheath instead of the reverse.

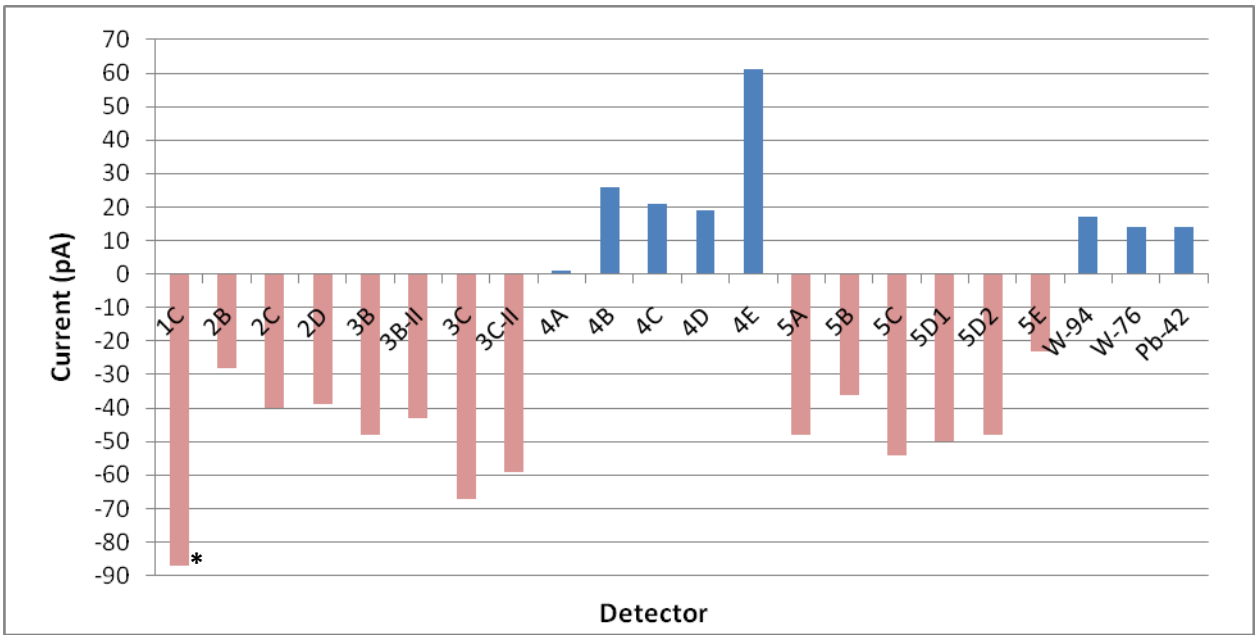

Figure 1: Magnitude of observed photocurrents from individual detectors in a 427 *Gy/h* gamma field. Detector 1C (*****) was irradiated in a 300 *Gy/h* field. Some detectors have been omitted due to the inability to determine a distinct photocurrent from the data.

3.2 Linearity of response

To ensure that the observed gamma signals were proportional to the gamma radiation field, a linearity check was performed using data collected by detectors 1C and 2C. The two detectors differ only in their length, and they were each exposed to a different gamma field. The sensitivities (per meter) of detectors 1C and 2C, respectively, were 9.67×10^{-13} $A{\bullet}m^{-1}(Gy/h)^{-1}$ and 9.37×10^{-13} $A{\bullet}m^{-1}(Gy/h)^{-1}$, a deviation of only 3%. The variation may be accounted for by the extra BNC connection between the detector and the coax cable in detector 1C.

In a CANDU reactor, where gamma fields are known to be able to reach as high as 5 *MGy/h*, these detectors should be able to produce signals on the order of hundreds of nanoAmperes. Such high signals are within range of currents produced by Vanadium and Pt-clad detectors that are currently deployed in large reactors [8].

3.3 Insulation resistance

Table 3 shows the internal resistance measured in each detector both inside and outside of a gamma radiation field. In absence of gamma radiation, there does not appear to be any relationship between internal resistance and detector size or insulation material. The lack of correlation may reflect the difficulty of construction. The two electrodes, ideally, should be kept in parallel, but when the core is not in parallel with the sheath or perfectly centered, regions develop where the two electrodes almost meet. These areas cause the internal resistance of detectors to plummet in proportion to the distance between the electrodes.

Table 3: Internal resistance of detectors in presence and absence of gamma radiation

Detector	*No Field* Internal Resistance (Ω)	*427 Gy/h* Internal Resistance (Ω)
1A	1.43E+10	---
1B	2.50E+08	---
1C	1.43E+08	---
2A	---	---
2B	---	---
2C	---	---
2D	1.43E+08	---
3A	1.07E+06	2.38E+06
3B	3.85E+09	3.51E+08
3C	2.16E+09	1.22E+09
3D	4.67E+10	1.72E+08
4A	2.53E+11	1.09E+09
4B	7.87E+07	1.12E+08
4C	1.35E+09	4.06E+08
4D	4.08E+07	4.61E+07
4E	9.71E+09	8.34E+08

Detector	*No Field* Internal Resistance (Ω)	*427 Gy/h* Internal Resistance (Ω)
5A	5.00E+10	4.72E+09
5B	1.00E+09	1.51E+09
5C	1.11E+07	9.59E+07
$5D_1$	2.00E+08	2.08E+08
$5D_2$	5.00E+07	5.96E+07
5E	---	6.97E+07
5F	---	1.64E+07
Thermo	5.00E+06	3.82E+06
W-94	2.00E+12	6.81E+11
W-76	3.33E+12	8.17E+11
Pb-42	2.00E+12	1.11E+12

Within a gamma radiation field, PbO-insulated detectors consistently exhibited greater internal resistance than alumina-insulated detectors. One possible explanation comes from the difference in ability of the oxides to capture atmospheric moisture. The internal resistance of early experimental detectors made with powdered oxides were reduced by decades with miniscule amounts of moisture capture [9]. Therefore, the higher internal resistance may be a result of the lesser tendency for PbO to absorb moisture compared to alumina.

The detectors filled with dried alumina did not consistently exhibit higher internal resistance than those filled with alumina that had not been dried. Due to the large surface area of powders, it is likely that the insulator absorbed water vapour during the short time it was exposed to the atmosphere while the detectors were being built. On the other hand, detectors in set 6 that were insulated by one solid piece of heat shrink produced the highest insulation resistance.

3.3.1 Effect on dynamic response

Figure 2 shows three types of irradiation curves that were observed when the detectors were irradiated. Type I curves are characterized by a prompt response to irradiation and a steady state signal that is quickly reached. Type II curves have a slightly delayed response that may stabilize after tens of minutes. Type III curves also exhibit a delayed response, but the signal decays significantly over time.

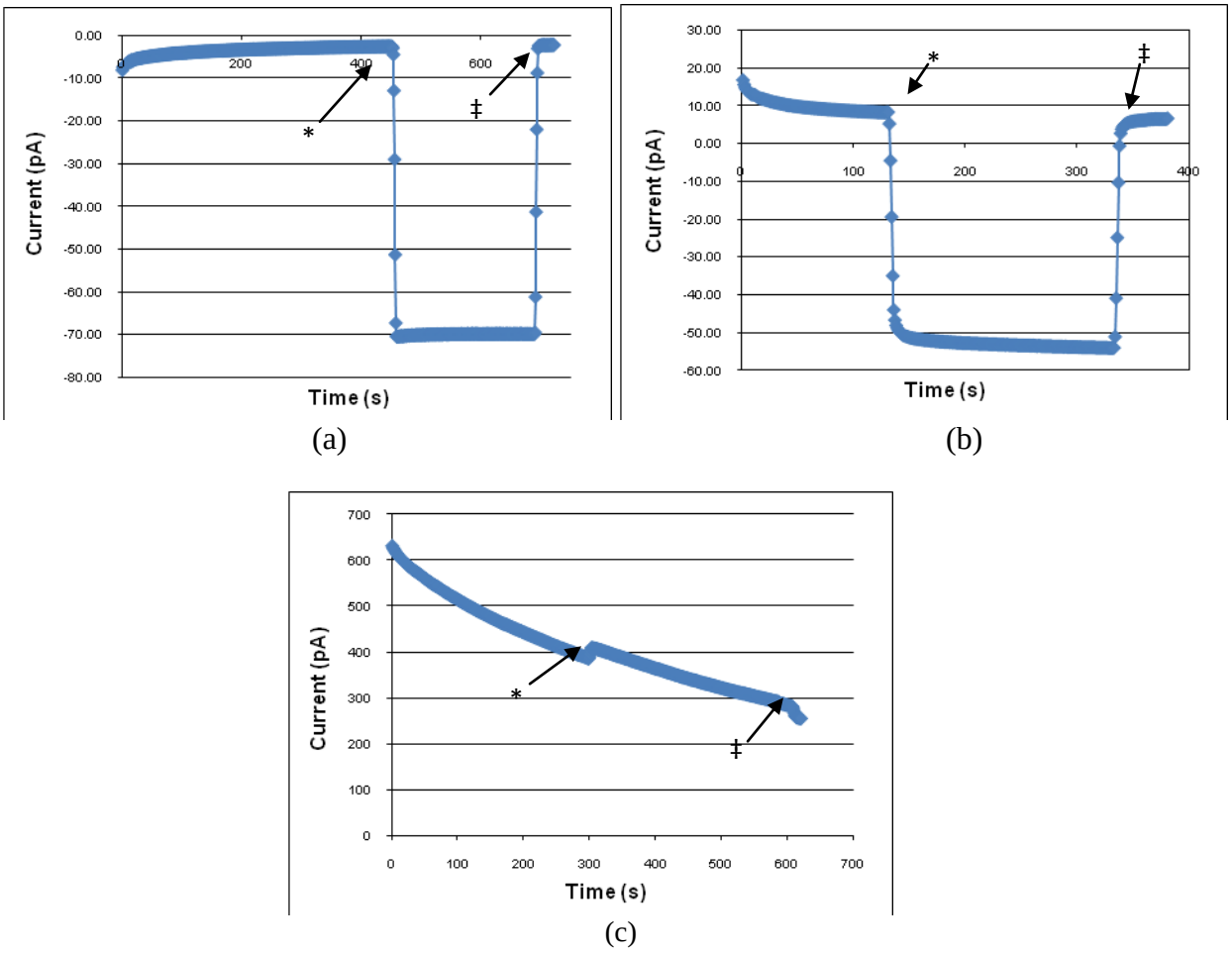

Figure 2: Types of signals produced as detectors were lowered into (*) and removed from (‡) the irradiation site. (a) Type I curve – prompt response and stable signal; (b) Type II curve – delayed response and somewhat stable signal; (c) Type III curve – delayed response and unstable signal.

Table 4 shows the dynamic response characteristics of all irradiated detectors. The most notable observation to be made is that Type I curves were generally produced by detectors that exhibited high insulation resistance ($> 10^9\ \Omega$). Detectors 5A and 5B were exceptions in that they generated Type II signals despite high internal resistance. On the other hand, detectors $5D_1$ and $5D_2$ had low internal resistance, yet they produced Type I signals. The results suggest that internal resistance may be a good indicator of the dynamic response of detectors with thick insulators (> 0.635 *mm*). As for detectors with thinner insulators, other properties, such as the dimensions of electrodes, may be a larger factor in determining signal type.

Table 4: Dynamic response characteristics of irradiated detectors

Type I	Type II	Type III
1C	1B	1A
2D	3B	3A
3C	3D	4D
4A	4B	5E
4E	4C	5F
$5D_1$	5A	Thermo
$5D_2$	5B	
W-94	5C	
W-76		
Pb-42		

In nuclear reactors, delayed signals are typically caused by neutron-induced nuclear transmutation either in the detector itself producing (n, β) currents, or inside the reactor fuel leading to delayed gammas producing (γ, e) currents in the detector. However, neutron-induced transmutation cannot occur in a gamma cell as there are no neutrons. The presence of delayed curves in present experiment suggests that there is a *third* mechanism by which delayed currents are produced in a self-powered flux detector. This mechanism is speculated to be the result of impurities present in the insulator caused by inadvertent exposure to air and moisture during assembly. These impurities ionize under radiation, introducing charge trapping centers and ion carriers that may delay electron release or slow electron transport. In this way, the dynamic response of detectors is a function of the sorption and packing structure of the powder insulator.

The ability to predict dynamic response of detectors does have practical value. Considering the functions of SPFDs, Type I signals would be ideal for all types of applications. Type II signals may be tolerated for flux mapping and spatial regulation of fuel rods, but it cannot be used in reactor trip mechanisms or other safety systems. On the other hand, Type III signals are unreliable for any purpose due to the long time required for the signal to stabilize.

3.3.2 Effect on noise signals

Unanticipated currents were observed when some detectors were connected to the FEMTO amplifier in absence of radiation. The phenomenon was not a tarring issue since the amplifier read currents on the order of 10^{-13} *A* before the detectors were attached. These signals,

however, are not random as their magnitudes correlate strongly with the insulation resistance of the detectors in a power relationship as seen in Figure 3.

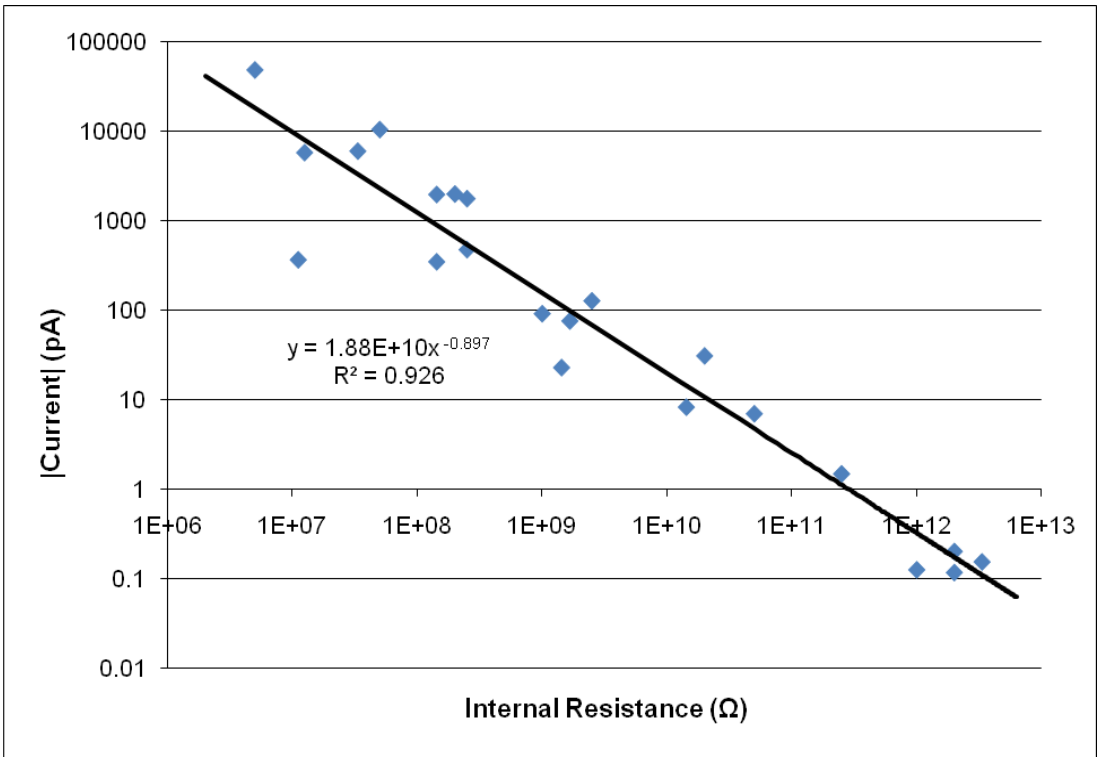

Figure 3: Relationship between the internal resistance of a detector and its corresponding signal in absence of a gamma field.

The relationship between the observed current and the internal resistance could be simplified by approximating the slope of the line as -1, yielding the equation for Ohm's Law. The constant in this equation implies that an offset voltage of approximately 0.02V was present across the terminals of the measuring circuit. Given that the FEMTO amplifier does have bias generating capabilities, the existence of such a small current is entirely possible. The importance of high insulation resistance within self-powered flux detectors is reinforced by this relationship.

Because the polarities of the unirradiated current do not consistently agree with that of the gamma-induced signal, it could be inferred that the current was a result of noise-producing agents rather than radiation-induced mechanisms of the detectors. However, noise from the measuring equipment and the RG-174 coaxial cable are unlikely the sole cause of the observed currents. The RMS input noise generated by the FEMTO amplifier at 10^{10} *V/A* gain is only 5.3×10^{-12} *A* [10], and a 100 *mm* piece of the coax cable only produced a current of $\sim 2 \times 10^{-12}$ *A* when irradiated in a 300 *Gy/h* field.

4. Conclusion

The present study explored the feasibility of using Lead(II) oxide as the insulator and the emitter of a self-powered flux detector. Contrary to the hypothesis, using PbO as the emitter did not generate a proportionally higher signal than a material with less electron density (alumina). Instead, the ability for PbO to produce electrons was masked by the presence of a substance with even greater electron density than itself (stainless steel). Because Oxygen in the compound reduces the electron density of Lead metal by almost a factor of 2, PbO seized to act as the principle electron emitter in the experimental detectors.

On the other hand, PbO proved superior over alumina, which is currently used in conventional SPFDs, as an insulating material. PbO was able to protect the experimental detectors from impurities during the assembly stage and from inherent voltage biases of the circuitry during the experimentation. The implications of a better insulator are significant when considering the effects of insulation resistance on the dynamic response of gamma-induced currents.

5. Acknowledgements

I would like to thank Dr. John Hilborn for introducing me to such an innovative project and for sharing his wisdom with me all through the summer. I am also indebted to my supervisors, Dr. Bhaskar Sur, Dr. Guy Jonkmans, and Shuwei Yue, for their guidance, teachings, and encouragement, which had enabled me to accomplish all that I did. It was an honour for me to work with you all.

I would also like to extend a big thanks to everyone else in AECL who has given me support and who has contributed to the completion of this project. I would like to give special mention to my DRSA students, Jason Zhao and Catherine Gui, for helping me conduct several experiments. Lastly, this paper would not have been possible without the Deep River Science Academy, which has given me the opportunity to work on this amazing research project.

6. References

[1] J. W. Hilborn, "Self-powered neutron detectors for reactor flux monitoring", Nucleonics, Vol. 22, Iss. 2, 1964, pp. 69-74.

[2] D.P. McAllindon, A. Celli, and J.W. Hilborn, "Performance of in-core flux detectors in CANDU", Atomic Energy of Canada Limited, COG-95-258 (Rev.1), 1995.

[3] B. Sur, P. Kumli, J. P. Johnston, and P. D. Tonner, "Determining prompt fractions of in-core flux detectors during full-power operation in CANDU", presented at the 20th Annual Conference of the Canadian Nuclear Society, Montreal, Quebec, Canada, 1999 May 20-June 2.

[4] R. B. Shields, "A platinum in-core flux detector", IEEE Transactions on Nuclear Science, Vol. 20, Iss. 1, 1973, pp. 603-608.

[5] J. W. Hilborn, Private conversation, Deep River, Ontario, Canada, 2009.

[6] F. W. Walker, J. R. Parrington, and F. Feiner. Nucleids and Isotopes: Fourteenth Edition. San Jose, CA: General Electric Company, 1989.

[7] B. Sur, Private conversation, Deep River, Ontario, Canada, 2009.

[8] B. Sur, "Introduction to in-core flux detectors (ICFD) in CANDU", presented at Atomic Energy of Canada Limited, Chalk River, Ontario Canada, 2008.

[9] W. Joslin, Email conversation, 2009.

[10] FEMTO Messtechnik GmbH, Variable Gain Low Noise Current Amplifier DLPCA-200 Datasheet, Berlin, Germany, 2009.